Phase coherence and the boson analogy of vortex liquids

A. K. Nguyen and A. Sudbø
Department of Physics, Norwegian University of Science and Technology, N-7034 Trondheim, Norway
(Received 22 December 1997; revised manuscript received 23 February 1998)

The statistical mechanics of the flux-line lattice in extreme type-II superconductors is studied within the framework of the uniformly frustrated anisotropic three-dimensional XY model. It is assumed that the externally applied magnetic field is low enough to invalidate the lowest Landau-level approach to the problem. A finite-field counterpart of an Onsager vortex-loop transition in extreme type-II superconductors renders the vortex liquid phase incoherent when the Abrikosov vortex lattice undergoes a first-order melting transition. For the magnetic fields considered in this paper, corresponding to filling fractions f given by $1/f = 12,14,16,20,25,32,48,64,72,84,96,112$, and 128, the vortex liquid phase is not describable as a liquid of well-defined field-induced vortex lines. This is due to the proliferation of thermally induced closed vortex loops with diameters of the order of the magnetic length in the problem, resulting in a ''percolation transition'' driven by non-field-induced vortices also *transverse* to the direction of the applied magnetic field. This immediately triggers flux-line lattice melting and loss of phase coherence along the direction of the magnetic field. Due to this mechanism, the field-induced flux lines lose their line tension in the liquid phase, and cannot be considered to be directed or well defined. In a nonrelativistic two-dimensional boson-analogy picture, this latter feature would correspond to a vanishing mass of the bosons. Scaling functions for the specific heat are calculated in zero and finite magnetic field. From this we conclude that the critical region is of order of 10% of T_c for a mass anisotropy $\sqrt{M_z/M}=3$, and increases with increasing mass anisotropy. The entropy jump at the melting transition is calculated in two ways as a function of magnetic field for a mass anisotropy slightly lower than that in $YBa_2Cu_3O_7$ (YBCO), namely, with and without a T-dependent prefactor in the Hamiltonian originating at the microscopic level and surfacing in coarse-grained theories such as the one considered in this paper. In the first case, it is found to be $\Delta S = 0.1 k_B$ per pancake vortex, roughly independent of the magnetic field for the filling fractions considered here. In the second case, we find an enhancement of ΔS by a factor that is less than 2, increasing slightly with decreasing magnetic field. This is still lower than experimental values of $\Delta S \approx 0.4 k_B$ found experimentally for YBCO using calorimetric methods. We attribute this to the slightly lower mass anisotropy used in our simulations. [S0163-1829(98)02329-7]

I. INTRODUCTION

The physics of vortex matter represents a new field of research that has opened up after the discovery of large fluctuation effects in the extreme type-II high-T_c superconductors. In particular, the work of Gammel *et al.*[1] and Nelson[2] were important milestones in the field, suggesting for the first time that the Abrikosov vortex lattice might melt *well below* the zero-field critical temperature. This extension of ideas originally proposed by Eilenberger[3] has proved to be fruitful. The melting of the flux-line lattice (FLL) well below the upper critical field crossover line due to large anisotropy combined with extreme nonlocality of vortex-vortex interactions,[4] as well as its first-order character, are now well established both on theoretical and experimental grounds. Nonetheless, the nature of the molten phase remains tantalizingly elusive. Obviously, there exists a two-dimensional (2D) boson analogy picture of the low-temperature phase of the FLL, where the corresponding boson system is an insulating one. This is nothing but Abrikosov's mean-field solution to the problem.[5] There is, however, mounting analytical and numerical evidence that a similar, intuitively appealing, picture of the molten phase via a 2D *nonrelativistic* superfluid boson system[2] may need a substantial revision.[6–10] As far as experimental results are concerned, the situation also appears quite intriguing.[11]

At issue here is to what extent the well-defined flux lines of the low-temperature FLL phase retain their integrity in the high-temperature molten phase. In this paper, we address the issue of the character of the vortex liquid via extensive Monte Carlo simulations of the uniformly frustrated 3D XY model.

An issue of fundamental importance is whether or not a vortex liquid (the molten phase of the FLL) is a superconductor or not when the vortex system is not pinned. It is clear that the superfluid response to a current applied transversely to the field-induced vortices is zero at all temperatures, provided that pinning is absent. In the perfect FLL there will, however, be a superfluid response to a current applied parallel to the magnetic field. There remains the possibility that a finite superfluid response might remain even in the liquid phase for this geometry, and that it may vanish only deep in the vortex liquid as suggested originally by Feigel'man *et al.*[12] A main point of this paper is to show that for the moderate mass anisotropy and large range of magnetic fields considered here, this in fact does not appear to be the case. Moreover, the reason that this is so has important consequences for the physical picture of the vortex liquid phase. Below, we give a summary of the main results of this paper.

The specific heat is calculated for filling fractions $f = 1/12, \ldots, 1/128, 0$, and the results are found to be in good agreement with the experimental results of Salamon *et al.*[13]

and more recent experiments of Roulin *et al.*[14] and Schilling and co-workers.[15,16] In particular, we find that the near-logarithmic singularity in zero magnetic field (the specific-heat exponent $\alpha=-0.007$) is converted to a broad crossover with a peak value suppressed rapidly compared to the zero-field case. This crossover defines, somewhat arbitrarily, the upper critical magnetic field. The entropy associated with the suppression of the specific heat at the crossover is partly compensated by the appearance of a δ function anomaly in the specific heat at temperatures well below the zero-field critical temperature. Such a δ-function peak is identified unambiguously with the first-order melting transition of the FLL. The field dependence of the temperature at which this appears defines the melting line of the FLL in the (B-T)-phase diagram of the superconductor. The field dependence of the entropy of the transition is found to be $\Delta S \sim B$, consistent with the suppression of the broad main crossover peak in the specific heat. This implies that the entropy per vortex per layer is essentially field independent in the field range and anisotropy range investigated here. We emphasize that the anisotropy considered, $\sqrt{M_z/M}=3$, is moderate and somewhat smaller than what is found in $YBa_2Cu_3O_7$ (YBCO). Nonetheless, the qualitative aspects of our results conform well with those found in YBCO.[15]

We find that in the field regime we have considered, i.e., fields down to $B\sim 1-5$ T, the melting of the vortex lattice is triggered by a proliferation of thermally induced closed vortex rings of order of the magnetic length of the system. This immediately leads to a ''percolation'' of vortex loops traversing the entire system in any given direction, and in particular in a direction perpendicular to the applied magnetic field. Hence, flux lines that are field induced will traverse the entire system as they weave their way from the bottom to the top of the system. In technical terms, in a simulation one needs to apply periodic boundary conditions at least once in the (x,y) directions before a flux line starting at the center of the bottom layer has reached the top layer. *Therefore, it does not make sense to view the vortex liquid phase as a collection of well-defined field-induced flux lines*. The above picture effectively means that the flux-line tension has vanished in the liquid phase. Within the 2D boson analogy picture, an equivalent statement would be that the boson mass, which is the analog of the line tension, has vanished.[17]

Scaling functions for the specific heat are calculated, in zero field as well as in finite field. From the regime where scaling is found in zero field, we find the width of the critical region to be $|T-T_c|/T_c\approx 0.1$ for a mass-anisotropy ratio $\Gamma=\sqrt{M_z/M}=3$. This is considerably wider than what one would naively obtain using the Ginzburg criterion. Moreover, this is slightly wider than what we have found for the isotropic case. The width of the critical region therefore increases slightly with mass anisotropy for the moderate values of Γ we have considered. Vortex loops are expected to be particularly important for the statistical mechanics of the FLL, provided that the melting line is found in the proximity of the critical region. From the obtained melting curve and the width of the critical region, we find that the melting curve crosses the critical region curve at a field of order $B=1$ T for $\Gamma=3$. Below this field, vortex loops will completely dominate the physics at the melting transition.

This paper is organized as follows. In Sec. II we present the model, the approximations involved, and the physical quantities considered, as well as an update of the procedure and the parameters used in our Monte Carlo simulations. In Sec. III we present and discuss detailed results for the filling fraction $f=1/20$. In Sec. IV we present results in a broad range of filling fractions $1/f\in[12,\ldots,128]$. Section V presents the conclusions of this paper.

II. MODEL

The phenomenological model considered in this paper for the high-T_c cuprates is the uniformly frustrated 3D anisotropic XY model on a lattice,[18–20,8,9] defined by the Hamiltonian

$$H\{[\theta(\mathbf{r})]\}=-\sum_{\mathbf{r},\mu=x,y,z} J_\mu \cos[\nabla_\mu\theta(\mathbf{r})-A_\mu(\mathbf{r})], \quad (1)$$

where θ is the local phase of the superconducting complex order parameter and ∇ is a lattice derivative. Furthermore, the coupling energy along the μ axis J_μ is defined by

$$J_x=J_y=\frac{\Phi_0^2 d}{16\pi^3\lambda_{ab}^2}\equiv J_\perp, \quad J_z=\frac{\Phi_0^2\xi_{ab}^2}{16\pi^3\lambda_c^2 d}.$$

Here Φ_0 is the flux quantum, ξ_{ab} is the superconducting coherence length within the CuO planes, and d is the distance between two CuO layers in *adjacent unit cells*. Furthermore, λ_{ab} and λ_c are the magnetic penetration lengths in the CuO planes and along the crystal's c axis, respectively. In Eq. (1), A_μ is related to the *quenched* vector potential $\mathbf{A}_{vp}$ by

$$A_\mu(\mathbf{r})\equiv\frac{2\pi}{\Phi_0}\int_{\mathbf{r}}^{\mathbf{r}+\hat{e}_\mu} d\mathbf{r}'\cdot\mathbf{A}_{vp}(\mathbf{r}'),$$

where $\hat{e}_\mu$ is the unit vector along the μ axis. This 3D XY model is dual to the anisotropic London model in the limit of $(\lambda_{ab},\lambda_c)\to\infty$.[21] This limit should be taken with the understanding that the coupling energies $J_\perp$ and J_z are maintained finite. When $(\lambda_{ab},\lambda_c)\to\infty$, gauge fluctuations are completely suppressed, leaving a quenched vector potential and uniform magnetic induction. Thus, the 3D XY model should give an adequate description of the physics of extreme type-II single-crystal superconductors in the field regime $B_{c1}\ll B\ll B_{c2}$. The condition $B_{c1}\ll B$ ensures that the contribution to the magnetic induction from individual flux lines overlaps strongly giving a uniform magnetic induction. The condition $B\ll B_{c2}$ ensures that details of the internal structure of the vortex cores are not essential. Moreover, the 3D XY model should give an adequate description of the physics of extreme type-II single-crystal superconductors in zero magnetic field when gauge fluctuations are not important.

In this paper we consider simple tetragonal systems with dimensions $L_x=L_y=L_\perp$ and L_z. The coordinate (x,y,z) axes are taken to be parallel to the crystal (a,b,c) axes, respectively. We measure the in-plane length scales (x,y,L_x,L_y) in units of ξ_{ab} and the length scales along the z axis $(z,\ L_z)$ in units of d. Our unit cell is a simple tetragonal system with dimensions $e_x=e_y=\xi_{ab}$, $e_z=d$. Periodic boundary conditions are used in all directions throughout.

A. Internal energy and specific heat

The specific heat per site C is obtained using the standard fluctuation formula

$$\frac{C}{k_B}=\frac{1}{L_\perp L_z}\frac{\langle H^2\rangle-\langle H\rangle^2}{(k_BT)^2}, \tag{2}$$

where k_B is Boltzmann's constant. Results for most temperatures are checked for consistency by differentiating the results for the internal energy with respect to temperature. To estimate the latent heat (entropy jump) at a first-order phase transition, we consider the internal energy per site E,

$$E=\frac{1}{L_\perp L_z}\langle H\rangle. \tag{3}$$

This expression holds as long as we do not include any T dependence in the Hamiltonian. Such a T dependence could conceivably arise in effective coarse-grained theories such as the Ginzburg-Landau theory, as first pointed out in Ref. 22. At a first-order phase transition there is a discontinuity in the internal energy per site ΔE associated with coexistence of the Abrikosov FLL phase and the vortex liquid. This in turn gives rise to a δ-function peak in the specific heat.[8,9] For the melting transition of a vortex line lattice, ΔE is related to the entropy jump per vortex lines per layer ΔS by

$$\frac{\Delta S}{k_B}=\frac{\Delta E}{fk_BT_m}, \tag{4}$$

where T_m is the melting temperature and f is the vortex-line density defined below in Eq. (8). For consistency, one may also check this result by extracting the entropy jump at the melting transition from the scaling of the height of the δ-function anomaly in the specific heat[23,8,9]

$$C=\text{const}+\frac{L^3}{4}\left(\frac{\Delta S}{k_BL^3}\right)^2. \tag{5}$$

B. Scaling functions for the specific heat

An issue of principle importance is whether or not closed thermally induced vortex loops, i.e., the critical fluctuations, will influence the melting of the FLL. Naively, one expects this to be the case provided that the melting temperature $T_m(B)$ is within the critical region of the zero-field transition. It is therefore a matter of interest to establish the width of the critical region of the anisotropic 3D XY model. To this end, we consider finite-size scaling of the specific heat. The region of data collapse of the specific heat evaluated at various system sizes identifies the width of the critical region. It is also of interest to find the extension of this critical region to finite fields, i.e., the width of the crossover region around the upper critical field, and how it depends on the anisotropy ratio Γ. If the melting line is located within this crossover region or close to it, one expects a vortex-loop ''blowout''[9,7] to dominate the physics at the melting transition, analogous to what was suggested to happen in superfluid He^4 by Onsager.[24] This is particularly important at very low magnetic fields, like those considered in the experiments of Zeldov *et al.*[11]

For the zero-field finite-size scaling of the specific heat, we have used cubic samples $L\times L\times L$ with $L=16,32,48,64,72,96$ to avoid spurious geometric effects. To investigate the possibility that the width of the critical region may depend on anisotropy, we have considered the two cases $\Gamma=1$ and $\Gamma=3$.

The finite-size scaling function for the specific heat may in general be obtained in standard fashion from the singular part of the free energy as[25,26]

$$C(t,L)=L^{\alpha/\nu}\Phi_\pm(|t|L^{1/\nu}),$$

or equivalently

$$\frac{C(t,L)}{C(t,\infty)}=G_\pm(|t|L^{1/\nu}),$$

where $|t|=|T-T_c|/T_c$, and where $\Phi_\pm(|t|L^{1/\nu})$ and $G_\pm(|t|L^{1/\nu})$ are analytic functions of their arguments. Here, α is the specific-heat critical exponent, and ν is the critical exponent of the superconducting correlation length; hyperscaling yields $\alpha=2-D\nu$ in a D-dimensional system. As discussed in detail in Ref. 26, a more convenient scaling form for numerical purposes is given by

$$\frac{C(t,L)-C(0,\infty)}{C(0,L)-C(0,\infty)}=G_\pm(|t|L^{1/\nu}). \tag{6}$$

We will use this scaling form to determine the width of the critical region.

In the presence of a general field X with scaling dimension $X\sim\xi^{-\lambda}$, where ξ is the correlation length $\xi\sim|t|^{-\nu}$, we have

$$C(t,X)=|t|^{-\alpha}\mathcal{G}_\pm(X|t|^{-\lambda\nu}).$$

Subtracting out the zero-field part, and introducing $y\equiv X|t|^{-\lambda\nu}$ and $\Delta C(t,X)\equiv C(t,X)-C(t,0)$, we find

$$|t|^\alpha\Delta C(t,X)=[\mathcal{G}_\pm(y)-\mathcal{G}_\pm(0)],$$

$$X^{\alpha/\lambda\nu}\Delta C(t,X)=y^{\alpha/\lambda\nu}[\mathcal{G}_\pm(y)-\mathcal{G}_\pm(0)]\equiv\mathcal{H}_\pm(y).$$

Choosing $X=B$, the induction, implies that the scaling dimension $\lambda=2$ when gauge fluctuations are suppressed, as is the case in the uniformly frustrated 3D XY model. Under such circumstances, the induction B will not acquire anomalous scaling. Hence, we obtain

$$B^{\alpha/2\nu}\Delta C(t,B)=y^{\alpha/2\nu}[\mathcal{G}_\pm(y)-\mathcal{G}_\pm(0)]\equiv\mathcal{H}_\pm(y), \tag{7}$$

where $y=B|t|^{-2\nu}$. We will use the above scaling form [Eq. (7)] to determine the width of the crossover region around the upper critical field as a function of B. Note, however, that this scaling form is not specific to the 3D XY model. By plotting appropriate ratios of temperature and field derivatives of these scaling functions, one may extract directly the critical exponents of the system as the slopes of the quantities being plotted; see, for instance, the very detailed analysis of this by Schilling and co-workers.[16] It is conceivable that such a procedure would yield a curve with a kink in it when $t>0$, as claimed to be observed by Schilling and co-workers. This in itself does not invalidate the 3D XY scaling of high-T_c cuprates. Conceivably, it could be due to a crossover from an XY fixed point to another fixed point, possibly with an

anomalously large value of $\nu \approx 1.5$, based on magnetization data. (Note that the specific-heat data of Schilling and coworkers in fact show an opposite trend, more consistent with a crossover to a Gaussian fixed point. This is to be expected if amplitude fluctuations of the order parameter were to dominate the phase fluctuations.) For more details, see the discussion below.

We note immediately that the above implies that $|t| \sim B^{1/2\nu}$ for finite fields, i.e., the width of the crossover region widens as B increases. Using the estimate $\nu = 2/3$ in three dimensions, we have $|t| \sim B^{3/4}$, implying that the crossover region around the upper critical on the low-temperature side has a positive curvature in the (B-T) phase diagram, which is also true for the melting curve, for which we have $|t|_M \sim B^{\eta}$, with $\eta \sim 2/3$. The widening of the crossover region is of course consistent with a broadening of the remains of the zero-field anomaly in the specific heat, to be calculated below.

The crossover curve $\tilde{B}(T < T_c)$ has a more rapid increase as a function of $T_c - T$ than the melting curve; recall the exponents 3/4 and 2/3, respectively. Due to the finite width of the zero-field critical region, there should then be a field regime where either the melting curve and the crossover curve intersect, or where the crossover curve is to the left of the melting curve in the B-T phase diagram. This depends on the width of the zero-field critical regime. Given the size of this regime, $|t| \leqslant 0.1$, the former scenario appears to us to be the more likely one, and this is also what we find in our simulations. Hence critical fluctuations, i.e., thermally induced vortex loops, should substantially influence the FLL melting in a finite regime of magnetic fields. From our simulations, to be presented below, we estimate the relevant field regime to be of order 0–1 T in an extreme type-II superconductor with $\Gamma = 3$.

C. Helicity modulus

As a probe of global superconducting phase coherence, we consider various helicity moduli Υ_x, Υ_y, and Υ_z. The helicity modulus Υ_μ along the μ direction is defined as the second derivative of the free energy with respect to a global phase twist along the μ direction;[19] explicitly, we obtain for the anisotropic uniformly frustrated 3D XY model

$$\Upsilon_\mu = \frac{1}{L_\perp L_z}\left\langle \sum_{\mathbf{r},\nu=x,y,z} J_\nu \cos[\nabla_\nu \theta(\mathbf{r}) - A_\nu(\mathbf{r})](\hat{e}_\nu \cdot \hat{e}_\mu)^2 \right\rangle - \frac{1}{k_B T L_\perp L_z}\left\langle \left[\sum_{\mathbf{r},\nu=x,y,z} J_\nu \sin[\nabla_\nu \theta(\mathbf{r}) - A_\nu(\mathbf{r})] \times (\hat{e}_\nu \cdot \hat{e}_\mu) \right]^2 \right\rangle .$$

When Υ_μ is finite, the system can carry a supercurrent along the μ direction. When Υ_μ vanishes, resistivity along the μ direction becomes finite. In systems with finite applied field along the z axis, we expect $\Upsilon_x = \Upsilon_y = 0$ for all temperatures in the continuum limit. In this case, any applied current along the xy plane will move the unpinned flux lines and dissipate energy. Discretization introduces a potentially singular perturbation by introducing an artificial pinning potential, the effect of which is more serious in a three-dimensional system than in a two-dimensional one. In the latter case, the effect of the potential may in principle be entirely avoided by considering low enough filling fractions,[27] whereas this is not possible in three dimensions in the thermodynamic limit. The size L_z of systems must therefore be tailored to the filling fraction f in order to avoid spurious pinning effects.

The thus introduced pinning potential will, at a low enough temperature, pin the flux lines in their positions, and cause $(\Upsilon_x, \Upsilon_y) \neq 0$ up to a depinning temperature T_d. To ensure that this artificially introduced pinning potential caused by the numerical lattice does not affect the FLL melting transition, we should consider systems with T_d much lower than all other ''critical'' temperatures of interest. T_d is controlled mainly by the filling fraction f; we have $T_d \to 0$ as $f \to 0$.[27,9] To adequately mimic the continuum limit of interest, low enough filling fractions must therefore be considered.

D. FLL structure function

To locate the position of the vortex elements we use the following procedure: The counterclockwise line integral of the gauge-invariant phase differences around any plaquette of the numerical lattice with surface normal along the μ direction must always satisfy

$$\sum_{C_i} j_\nu(\mathbf{r}) = 2\pi[n_\mu(\mathbf{r}) - f_\mu],$$

$$j_\nu(\mathbf{r}) = \nabla_\nu \theta(\mathbf{r}) - A_\nu(\mathbf{r}).$$

Here, C_i is the closed path traced out by the links surrounding an arbitrary plaquette, and ν represents the Cartesian components of the current in the directions of the links that comprise the closed path C_i. Furthermore, $j_\nu(\mathbf{r})$ is the current on the link between site $\mathbf{r}$ and site $\mathbf{r} + \hat{e}_\nu$ and $n_\mu(\mathbf{r}) = 0, \pm 1$ represents a vortex segment penetrating the plaquette enclosed by the path C_i. Here, f_μ is the vortex-line density along the μ direction, and is given by

$$f_\mu = \frac{\sum_{\mathbf{r}} n_\mu(\mathbf{r})}{L_\perp L_z}. \tag{8}$$

To probe the structural order of the vortex system, we consider the in-plane structure function for n_z vortex segments within the same plane,[2]

$$S(\mathbf{k}_\perp) = \frac{1}{f^2 L_\perp^4 L_z}\left\langle \sum_z \left| \sum_{\mathbf{r}_\perp} n_z(\mathbf{r}_\perp, z) e^{i\mathbf{k}_\perp \cdot \mathbf{r}_\perp} \right|^2 \right\rangle .$$

In the FLL phase we expect to see a periodic array of sharp Bragg peaks in the $\mathbf{k}_\perp$ plane. In the vortex liquid phase we expect to see Bragg rings with radius $k_\perp = 2\pi/a_v$ and $4\pi/a_v$, characteristic of a liquid. Here, a_v is the average distance between neighboring vortex lines.

E. Monte Carlo procedure

The Monte Carlo updating procedure used in this paper is the following. The numerical lattice is stepped through in a systematic manner. At each site a change of the local phase of the superconducting condensate is attempted by a random amount $\Delta\theta \in [-\pi,\pi\rangle$. The attempt is accepted or rejected according to the standard Metropolis algorithm.

If the accepted phase change causes the current on a link $j_\mu(\mathbf{r})$ to exceed the range $j_\mu(\mathbf{r}) \in [-\pi,\pi\rangle$, an amount $\pm 2\pi$ is added to the current such that $j_\mu(\mathbf{r})$ is brought back into the primary interval $j_\mu(\mathbf{r}) \in [-\pi,\pi\rangle$. An important point is that this operation can only generate a closed unit vortex loop around the link where the current is changed, thereby conserving the net induction of the system. No net vorticity is ever introduced by the procedure, and the procedure also guarantees that no vortex line can start or end within the sample. One sweep refers to $L_\perp^2 L_z$ attempts to change the phase angle.

We fix the height of our systems to $L_z=40$ and let $L_\perp$ vary from 40 to 128 depending on the flux-line density under consideration. In Refs. 8 and 9, it was noted that for systems with moderate anisotropy ($\Gamma\sim 3$), finite-size effects are rather small when the linear dimension of the system and the total number of flux lines exceed ~ 40. Thus, we believe that finite-size effects will not affect the conclusions in this paper. Likewise, it was observed by the same authors that finite-size effects were negligible when L_z was increased beyond $L_z=40$ for the anisotropy considered here, $\Gamma=3$. This has motivated our choice of $L_z=40$.

In this paper we fix the anisotropy parameter Γ to

$$\Gamma \equiv \sqrt{\frac{J_\perp}{J_z}} = \frac{\lambda_z d}{\lambda_{ab}\xi_{ab}} = 3$$

in most simulations. Occasionally, comparison is made for the isotropic case $\Gamma=1$. The magnetic field B is applied along the crystal c axis, giving a vortex-line density f,

$$f_x = f_y = 0, \quad f_z \equiv f = \frac{B\xi_{ab}^2}{\Phi_0}. \tag{9}$$

The flux-line densities f considered are $1/f=12$ (48), 14 (56), 16 (48), 20 (40), 25 (50), 32 (64), 48 (48), 64 (64), 72 (72), 84 (84), 96 (96), 112 (112), 128 (128), ∞ (64). The numbers in the parentheses denote $L_\perp$ for the corresponding vortex-line density. Note that we have chosen, with our gauge, $L_\perp$ for each filling fraction f in such a way that we ensure that an integer number of magnetic Brillouin zones will fit on the reciprocal lattice of each system, enabling us to use periodic boundary conditions in the x,y directions. As will be observed, $L_\perp$ is an integer multiple of $1/f$ in each case.

The value of f is prescribed by loading the following phase-difference pattern onto the numerical lattice (using Landau gauge), a system with $\theta(\mathbf{r})=0$ for all $\mathbf{r}$,

$$A_y(x,y,z) = 2\pi f x.$$

The system is then heated to a temperature well above any transition/crossover temperatures of interest, at which point slow cooling is started. The filling fraction f is conserved by our Monte Carlo procedure, and the moves are carried out on the gauge-invariant phase differences on each link. Note that we do not need to *assume* any ground-state configuration by this procedure. Extremely long simulations, typically 4×10^6–6×10^6 sweeps, are, however, required in order to capture the correct physics at the FLL melting transition and to reveal any δ-function anomalies in the specific heat at the melting transition, particularly at low filling fractions.

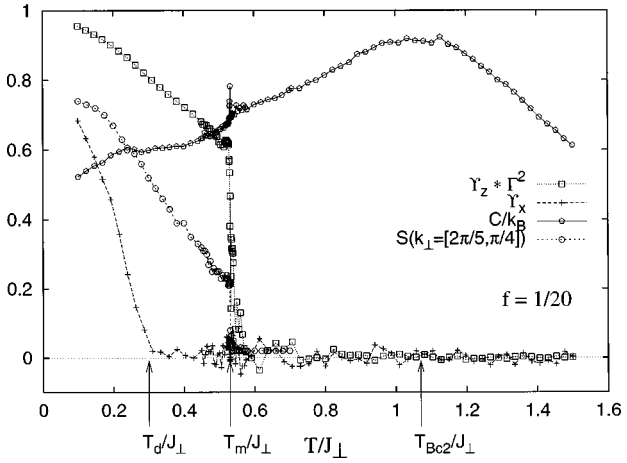

FIG. 1. Specific heat C per site, in-plane structure factor $S(\mathbf{k}_\perp = 2\pi/5,\pi/4)$, helicity modulus along z axis Υ_z, and helicity modulus along x axis Υ_x as functions of temperature for the system with vortex-line density $f=1/20$. The in-plane structure function $S(\mathbf{k}_\perp)$ jumps discontinuously from 0.2 to 0 precisely at $T_m=0.531J_\perp$ indicating that the FLL melts in a first-order phase transition. At the same temperature, Υ_z also shows a discontinuity from 0.6 to 0, indicating that *the FLL melts directly into the incoherent vortex liquid* with no global phase coherence along the applied magnetic-field direction. At temperatures above T_m there is no global phase coherence in any direction. The specific heat also shows a δ-function anomaly, precisely T_m. The broad specific-heat anomaly at $T_{Bc2}\sim 1.05J_\perp$ represents the remains of the zero-field Onsager vortex loop blowout. Note that for temperatures $T_m<T<T_{Bc2}$ local superconducting phase coherence still exists, giving strong diamagnetic fluctuations in the liquid phase. The FLL depins from the numerical lattice at $T_d \ll T_m$, where Υ_x vanishes. Thus, the FLL melting transition at $T_m \gg T_d$ is not affected by the numerical lattice.

III. RESULTS: $f=1/20$

A. FLL melting and phase coherence

To identify the possible different phases and phase transition(s)/crossover(s) in a system with finite flux-line density, we first concentrate on results for the system $f=1/20$. *Similar results are found in all other finite flux-line densities considered in this paper*, to be detailed below. We have measured temperatures in units where $k_B=1$.

Figure 1 shows the specific heat per site C, the helicity modulus along the applied-field direction Υ_z, the helicity modulus perpendicular to the applied-field direction Υ_x, and the in-plane structure function $S(\mathbf{k}_\perp)$ as functions of temperature. Figure 1 shows that the in-plane structure function $S(\mathbf{k}_\perp=2\pi/5,\pi/4)$ has a sharp drop from 0.2 to 0 precisely at $T_m=0.531J_\perp$, indicating that the FLL melts at T_m in a first-order phase transition. For a more global view, Fig. 2 illustrates the density plot of $S(\mathbf{k}_\perp)$ for $k_x,k_y \in [-\pi,\pi]$ at four different temperatures; $T/J_\perp=0.450$, 0.530, 0.531, 0.532.

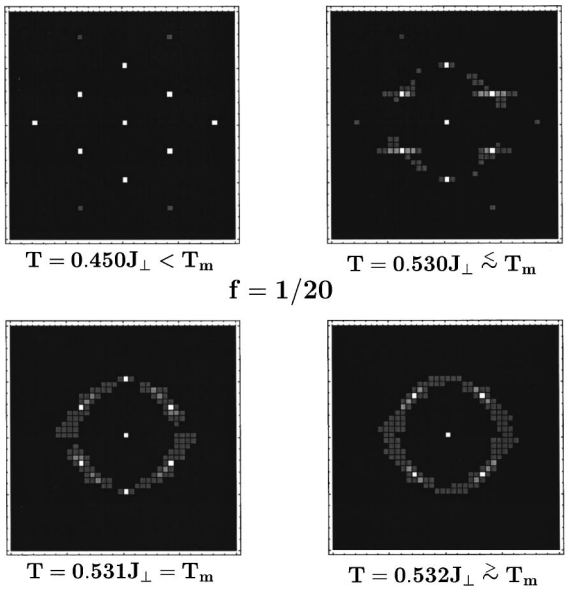

FIG. 2. Intensity plots of the structure function $S(\mathbf{k}_\perp)$ for various temperatures for the system with flux-line density $f=1/20$. $k_x \in [-\pi,\pi]$ and $k_y \in [-\pi,\pi]$ are along the horizontal and the vertical direction, respectively. The brightness in the plots is a measure of the magnitude of $S(\mathbf{k}_\perp)$. To enhance features we put all points where $S(\mathbf{k}_\perp)<0.01$ (noise level) to black and all points where $S(\mathbf{k}_\perp)>0.05$ to white. Precisely at T_m, the sharp Bragg peaks in $S(\mathbf{k}_\perp)$ are converted into Bragg rings, characteristic of a liquid. Thus, the FLL melts into a vortex liquid within a temperature region of $\Delta T=0.001J_\perp$.

It is clearly seen that the periodic array of sharp Bragg peaks is converted into a ring precisely at $T_m=0.531J_\perp$, within a narrow temperature region of $\Delta T=0.001J_\perp$ around T_m.

To clarify whether the phase coherence along the direction of the applied magnetic field is finite in the vortex liquid phase, we consider the helicity modulus along the z axis Υ_z. In Fig. 1 it is clearly seen that Υ_z shows a sharp jump from 0.6 to 0 at T_m precisely where the FLL melts. This shows that the FLL melts directly into an *incoherent vortex liquid* in a first-order phase transition. We will return to this important point later, since it has important consequences for the physical picture of the vortex liquid phase. The above result is in complete agreement with the work of Ref. 8 using the 3D XY model, the work of Ref. 22 using the lowest Landau-level approximation, and earlier work by us using the 3D anisotropic Villain model.[9] In all these works, it was found that longitudinal phase coherence is lost as soon as the vortex lattice melts in the thermodynamic limit. We emphasize that opposite conclusions were drawn in earlier work by us and others.[7,19,29] We believe that this discrepancy may be due to one or several of the following three factors: (i) In earlier work, the system size in the z direction may not have been large enough, particularly for the isotropic case, (ii) the simulations were not run for a long enough time, and (iii) the results were obtained upon heating only. Our more recent results in Ref. 9 and in the present paper are obtained upon heating *and* cooling.

A first-order phase transition is manifest in the form of a δ-function anomaly in the specific heat. From the height of this anomaly one may deduce the latent heat of the transition.

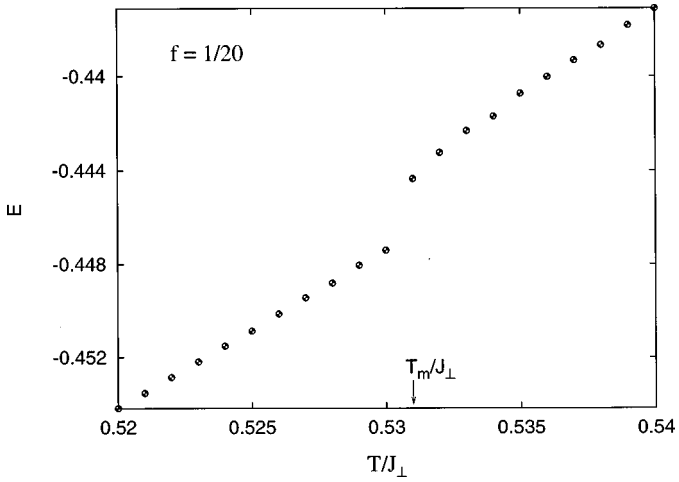

FIG. 3. Internal energy per site E as a function of temperature for the system with vortex line density $f=1/20$. The data are obtained from a cooling sequence using 3 000 000 sweeps per temperature. The internal energy has a discontinuous jump at T_m indicating a first-order transition from an ordered state (FLL) to a disordered state (phase-incoherent vortex liquid). This jump in the internal energy is used to determine the latent heat (entropy jump) at the FLL melting transition. The jump in E here corresponds to a jump in the entropy per vortex line per layer $\Delta S(f=1/20)=0.1k_B$.

Figure 1 shows that the anomaly occurs at $T_m=0.531J_\perp$, precisely where the structure function and the helicity modulus vanish. These results are in complete agreement with those of Ref. 8 obtained on the uniformly frustrated 3D XY model for $f=1/25$, as well as those found in Ref. 9 using the uniformly frustrated 3D anisotropic Villain model for $f=1/32$. Below we consider filling fractions down to $f=1/128$, finding that these results still hold.

The latent heat of the first-order FLL melting transition at T_m is obtained from the jump in the internal energy shown in Fig. 3 using Eq. (4). Here, the entropy jump per vortex line per layer is estimated to be $\Delta S=0.1k_B$. To obtain the spike in the specific heat we must (i) ensure that the transition temperature is located very accurately, typically to within one part in 10^3 and (ii) increase the simulation length to at least 6 000 000 sweeps over the lattice for each temperature. The extreme length of the simulations is necessary to allow the system to switch back and forth between the ordered phase and disordered phase at the phase transition an adequate number of times, typically at least ten times.

B. Breakdown of the 2D boson analogy

The specific heat has a broad anomaly at $T_{Bc2}\simeq 1.05J_\perp \gg T_m$, indicating a crossover. This broad crossover was unambiguously identified in our previous work as the remains of a zero-field Onsager vortex loop ''blowout''[7,9] that destroyed superconductivity on all length scales. However, since the remains of the zero-field vortex loop ''blowout'' takes place first at $T_{Bc2}\gg T_m$, superconductivity still exists locally in finite domains in the incoherent vortex liquid phase, giving strong diamagnetic fluctuations.[20] Since the global phase coherence in all directions is destroyed in the incoherent vortex liquid phase, the superfluid stiffness is zero

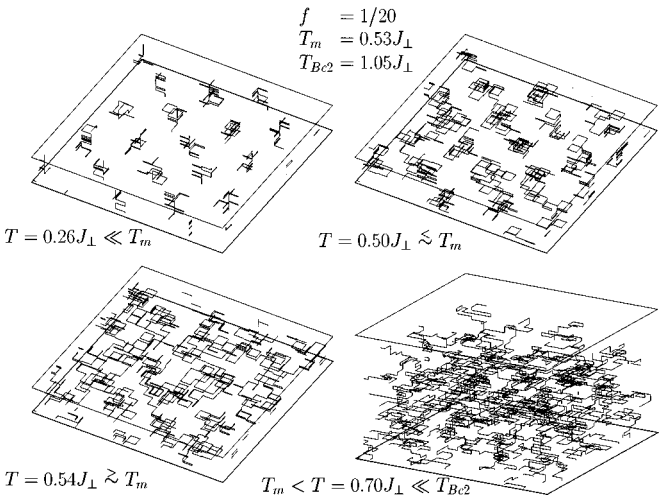

FIG. 4. Snapshots of the vortex configuration for the system with vortex-line density $f=1/20$ for four temperatures, $T/J_\perp = 0.26,0.50,0.54,0.70$. For clarification we have shown only a part of the system; $x,y \in [0:20]$ and $z \in [0:40]$. For $T=0.26J_\perp \ll T_m$, the flux lines form a hexagonal lattice. Although there are many thermally induced defects attached to each flux line, they are nonetheless well-defined quantities. For $T=0.50J_\perp \lesssim T_m$, the FLL is still intact. Although the flux lines now contain many larger defects, they are still well defined. For $T=0.54J_\perp \gtrsim T_m$, the FLL has melted. For $T \gtrsim 0.54J_\perp$, it is seen that the flux lines are no longer well-defined quantities. There exists at least one way for a flux line to thread the system in any direction. For any vortex configuration, therefore, there exists at least one flux line threading the sample in the direction perpendicular to the magnetic field.

in all directions in this phase, and any applied current through the system will dissipate energy. Thus, in the incoherent vortex liquid phase the system has both finite resistivity in all directions, as well as strong diamagnetic fluctuations.

The numerical lattice is a singular perturbation in a three-dimensional system, and one may ask whether the first-order FLL melting transition at T_m is affected by the artificially introduced pinning potential. To address this issue we consider the helicity modulus along the x axis Υ_x. In Fig. 1, it is seen that the helicity modulus along the x axis Υ_x drops to zero already at $T_d=0.1J_\perp \ll T_m$. From this we conclude that above T_d the system exhibits a ''floating solid'' phase.[27] Thus the FLL melting transition at T_m is *not* affected by the pinning potential caused by the numerical lattice.

Snapshots of the FLL, the incoherent vortex liquid phase, and the normal metal phase of the system $f=1/20$ for four temperatures $T/J_\perp = 0.26$, 0.50, 0.54, 0.70 are shown in Fig. 4. For clarity only a part of the system, $x,y \in [0:20], z \in [0:40]$, is shown. For the system $f=1/20$, we have found $T_m=0.53J_\perp$ and $T_{Bc2}=1.05J_\perp$. For $T=0.26J_\perp \ll T_m$, the flux lines form a hexagonal lattice. Although there are many thermally induced defects attached to each flux line, they remain well-defined entities. For $T=0.50J_\perp \lesssim T_m$, though the flux lines now fluctuate substantially, they nonetheless remain intact. So does the FLL, as evidenced by the results for the structure function; see Figs. 1 and 5. For a slightly more elevated temperature $T=0.54J_\perp \gtrsim T_m$, the FLL has melted. A key observation is that, immediately upon melting, the flux lines are no longer well-defined entities; there are

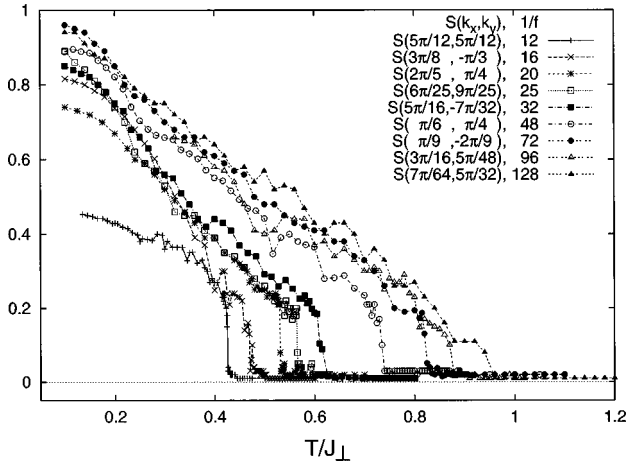

FIG. 5. The in-plane structure function $S(\mathbf{k}_\perp)$ as a function of temperature for several vortex-line densities f. For a given f, $S(\mathbf{k}_\perp)$ with the corresponding value of $\mathbf{k}_\perp$ shows a sharp drop from ~ 0.2 to 0 at a well-defined FLL melting temperature $T_m(f)$.

many intersections between flux lines, vortex loops have proliferated, and there exists at least one way to percolate from one side of the sample to the opposite side in any direction. Thus, for any given direction there always exists at least one ''infinitely'' long vortex line perpendicular to it, and any applied current will move these ''perpendicular'' vortex lines and dissipate energy. Note that in this picture vortex lines in the incoherent vortex liquid cannot be described as world lines of 2D *nonrelativistic* bosons.[2] Thus, one vortex line in the center of the system will meander all the way to the boundary surface (with surface normal perpendicular to the applied-field direction) and back as a field-induced flux line weaves its way from the bottom to the top of the system. This corresponds to zero flux-line tension, and a wandering exponent ζ of the flux line that is $\zeta \geqslant 1$ or, equivalently, zero bosonic mass in the 2D boson analogy.

Note that the 2D quantum boson system we have in mind when referring to the work of Ref. 2 is a nonrelativistic system. The picture we have in mind for the liquid phase is more akin to a *relativistic* 2D quantum boson system, where the proliferation of vortex loops and overhangs in the flux lines corresponds to vacuum fluctuations in the boson system. This connection has been nicely exposed in Ref. 28.

IV. RESULTS: $1/f \in [12,\ldots,128]$

A. Structure function $S(\mathbf{k}_\perp)$

We show in Fig. 5 the in-plane structure function $S(\mathbf{k}_\perp)$ as a function of temperature for several vortex line densities f; $1/f=12(\mathbf{k}_\perp=5\pi/12,5\pi/12)$, $16(\mathbf{k}_\perp=3\pi/8,-\pi/3)$, $20(\mathbf{k}_\perp=2\pi/5,\pi/4)$, $25(\mathbf{k}_\perp=6\pi/25,9\pi/25)$, $32(\mathbf{k}_\perp=5\pi/16, -7\pi/32)$, $48(\mathbf{k}_\perp=\pi/6,\pi/4)$, $72(\mathbf{k}_\perp=\pi/9,-2\pi/9)$, $96(\mathbf{k}_\perp=3\pi/16,5\pi/58)$, $128(\mathbf{k}_\perp=7\pi/64,5\pi/32)$. For a given vortex line density, $S(\mathbf{k}_\perp)$ with the corresponding value of $\mathbf{k}_\perp$ shows a sharp drop from ~ 0.2 to zero defining a field-dependent FLL melting temperature $T_m(f)$. This clearly shows that, for all values of f considered here, the FLL melts in a first-order phase transition. For decreasing f, the transition temperature $T_m(f)$ increases towards T_c as expected; see Fig. 7.

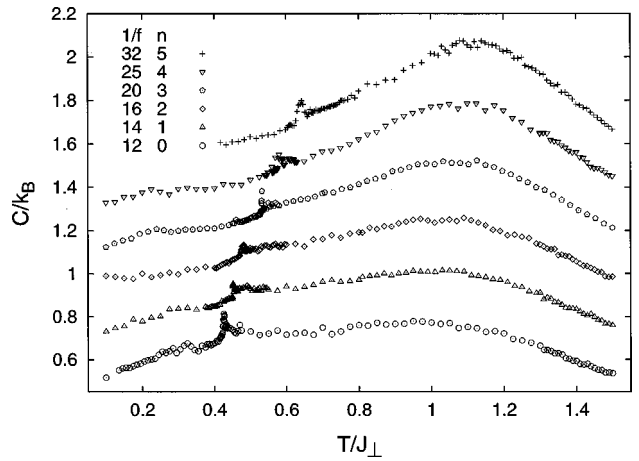

FIG. 6. Monte Carlo results for the specific heat per site of the anisotropic 3D XY model as a function of temperature for several vortex-line densities f. The system sizes depends on filling fraction, as explained in the text, and $\Gamma=3$. For clarity the nth curves are shifted by an amount $0.2n$ upwards. For each f there is a spike at a f-dependent critical temperature $T_m(f)$ indicating a first-order phase transition.

B. Helicity modulus along the field direction Υ_z

In Fig. 6 the helicity modulus Υ_z along the direction of the magnetic field is shown as a function of temperature for the same set of flux-line densities as for the case of the in-plane structure function. As f is varied, Υ_z shows a sharp drop towards zero precisely at the corresponding FLL melting temperature $T_m(f)$. Thus, we may conclude that for all filling fractions considered, the FLL melts directly into an incoherent vortex liquid. The temperature region where the vortex liquid and the phase coherence along the applied field coexist, found previously by several authors,[19,20,7,12] is not found for any flux-line density f considered in this paper. We believe that the temperature regime, where the vortex liquid exists with phase coherence along the field direction, pertains to thin-film geometries, or it is otherwise an artifact of short simulations and hysteretic behavior in the heating/cooling sequence of the vortex system. The phase-coherent vortex liquid does not exist in the thermodynamic limit of an equilibrium system, at least in systems with moderate anisotropy and moderate magnetic induction. The possibility of the existence of a very small magnetic-field induction B_{lower} [dependent on the anisotropy $B_{lower}(\Gamma)$] below which the phase coherence along the field direction can exist in the vortex liquid is not completely ruled out by this work.

Note that $T_m(f)$ is correlated with the temperature where the corresponding Υ_z starts to fall sharply towards zero, not the lowest temperature where Υ_z vanishes. One may question whether it is correct to take the temperature where Υ_z starts to show a sharp drop as the temperature where phase coherence along the applied field vanishes. For moderate vortex-line densities this poses no problem, since the drop in Υ_z is very sharp. However, for $f<1/48$, the transition extends over a small temperature region. By experience, we know that when the system size and the number of vortex lines in the system increase, the drop in Υ_z sharpens and the tail in Υ_z disappears. We believe therefore that this tail is only a finite-size effect.

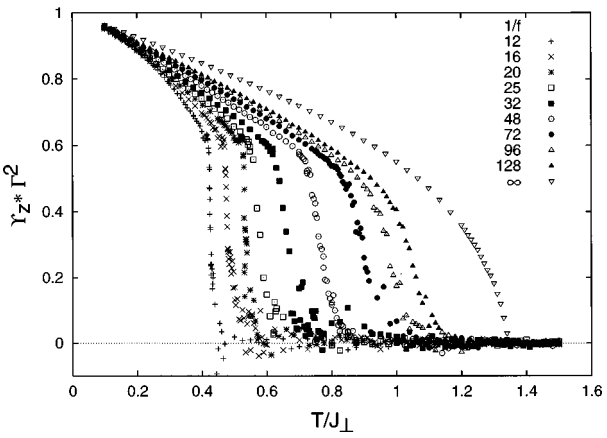

FIG. 7. The helicity modulus Υ_z along the field direction as a function of temperature for several flux-line densities f. For all densities, Υ_z shows a sharp drop towards zero precisely at the corresponding FLL melting temperature $T_m(f)$. Thus, the FLL melts directly into an incoherent vortex liquid.

The main conclusion of the above discussion is that in the thermodynamic limit, no phase coherence exists in the vortex liquid phase. This conclusion is consistent with mounting evidence from numerical simulations,[8,9,30] obtained however only in a limited filling range $1/f\in$ [25–36]. Our present results extend this conclusion to much lower filling fractions.

C. Specific heat

For all filling fractions down to $f=1/32$, we have found a δ-function anomaly in the specific heat at $T_m(f)$, indicating a first-order phase transition; see Fig. 7. For smaller filling fractions $f\leqslant 1/48$ we find no clear evidence of a spike in the specific heat. Note that in passing from the system with $f=1/32$ to the system with $f=1/48$, the number of field-induced flux lines is reduced from 128 to 48. We believe that the observed ''nonexistence'' of the δ-function anomalies at the FLL melting temperature in the system with very low flux-line densities is attributable to two factors: (1) for the system with $f\leqslant 1/48$ we have too few field-induced vortex lines in our systems and (2) the contribution to the specific heat from the field-induced flux lines for these filling fractions is too small compared to the ''spin-wave'' and vortex-loop contributions to be detected by our simulations.

In Fig. 8, we show the specific heat as a function of temperature for the same set of corresponding system sizes and flux-line densities as previously used in calculating the in-plane structure function and the helicity modulus along the direction of the applied magnetic field. For decreasing f the crossover temperature $T_{Bc2}(f)$ increases and moves towards the zero-field critical temperature $T_{Bc2}(f=0)=T_c$. The broad anomaly in the specific heat sharpens and the maximum height of the cusp increases, evolving smoothly towards the zero-field specific-heat singularity at T_c. T_{Bc2} denotes the crossover temperature at which the remains of the zero-field vortex-loop ''blowout'' takes place. In a finite magnetic field the vortex-loop ''blowout'' at $T_{Bc2}(f)$ causes only a crossover and the actual phase transition takes place at a lower temperature $T_m(f)$, where the FLL undergoes a first-

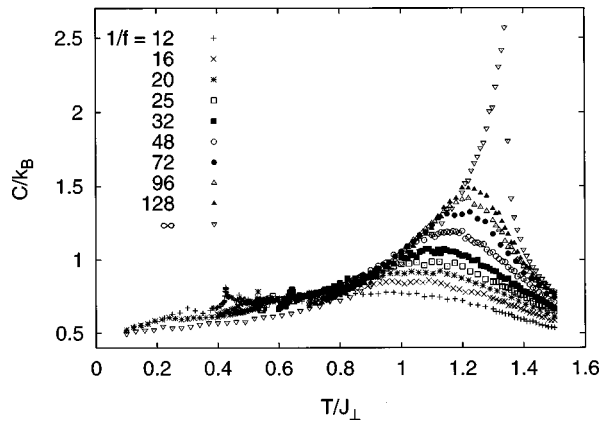

FIG. 8. Monte Carlo results for the specific heat of the anisotropic 3D XY model as a function of temperature for several flux-line densities. For decreasing f (decreasing magnetic-field induction B) the crossover temperature $T_{Bc2}(f)$ increases and moves towards the zero-field critical temperature $T_{Bc2}(f=0)=T_c$. The broad anomaly (cusp) in the specific heat becomes sharper and the maximum height of the cusp increases. Thus, for decreasing f the specific heat evolves smoothly to the zero-field specific-heat singularity at T_c. The spike in the specific heat at $T_m(f) \ll T_{Bc2}(f)$ in each graph is hidden in the noise of the other graphs and is therefore hard to recognize in this particular figure. While in zero magnetic field the vortex loop blowout is the mechanism for the second-order phase transition at T_c, in finite magnetic field the vortex loop blowout at $T_{Bc2}(f)$ is only a crossover. The phase transition in systems with finite vortex-line densities takes place at a lower temperature $T_m(f)$, where the vortex-line lattice melts.

order melting transition triggered by a proliferation of vortex loops with diameters at least of the order of the magnetic length in the system.

Scaling functions for the specific heat both for zero field and finite field are shown in Figs. 9 and 10. For the zero-field case, using Eq. (6), it is seen from Fig. 9 that data collapse is obtained over a wide region out to values of the scaling variable $|t|L^{1/\nu}>10$ for $L \geqslant 32$ on the low-temperature side of T_c. Note also that the width of the scaling regime is slightly larger for $\Gamma=3$ than for $\Gamma=1$. We expect this trend to persist with increasing Γ; in the extreme case where the layers may be considered completely decoupled, i.e., $\Gamma \to \infty$, the entire low-temperature regime is known to be critical.[31] For smaller L, it appears from our simulations that we do not obtain scaling. Using the value $\nu=0.669$,[26] we find that the width of the critical region is given by $|t| \approx 0.1$.

The critical scaling of the specific heat is also considerably better above T_c than below. This is due to the fact that vortex loops, i.e., the critical fluctuations, to a much larger extent dominate the free energy above T_c compared to below T_c. Below T_c there is a nonsingular contribution to the free energy, and hence specific heat, due to spin-wave fluctuations of the local phase of the order parameter.

The scaling function of the specific heat in a finite field, given above in Eq. (7), is also calculated for filling fractions f given by $1/f=12,16,20,25,32,48,72,96,128$ with correponding system sizes identical to those used for the structure function above. The anisotropy is $\Gamma=3$. The scaled results are in good agreement with the works of Salamon *et al.*,[13] Roulin *et al.*,[14] and Schilling and co-workers.[16] Note that while Ref. 16 makes the point that 3D XY scaling does not appear to describe well the experimental results above T_c in single-crystal $YBa_2Cu_3O_7$ in the field range 0.75–7 T, it does appear to work well below T_c. The reason for this may be that for an optimally doped compound, the temperature at which a pseudogap opens up may not be much higher than the T_c at which phase coherence is established. The results are therefore likely to be influenced by amplitude fluctuations above T_c. This should not be the case below T_c. Hence, we believe that the field range considered is not the only issue; there is also the observation of a crossover from an XY critical point to a Gaussian critical point when increasing the temperature above T_c, approaching a mean-field-like temperature T_{MF} where preformed pairs start to dissociate. An obscuring factor is that the specific-heat data and magnetization data of Schilling and co-workers show opposite trends in their deviation from XY scaling. Note that the analysis of Ref. 16 is *not* specific to the XY model; the scaling forms that are used are quite general. Were the temperature scales T_c and T_{MF} well separated, XY critical scaling would presumably persist above T_c. This would, for instance, be the case in *underdoped* cuprates.[32]

At any rate, it is the width of the critical region *below* T_c that is of interest in establishing the importance of interplay between vortex loops and FLL melting. The width of the critical region should increase with underdoping, and hence the interplay between vortex loops and FLL melting is expected to be more pronounced when the cuprates become more underdoped.[32]

We note that the scaling is better above T_c than below, again because nonsingular contributions to the free energy, in this case also arising from the FLL, contribute significantly. The spikes in the finite-field scaling function are due to the specific-heat anomalies at the FLL melting transition.

D. Entropy discontinuity at the FLL melting transition

The latent heat, or equivalently the discontinuity in entropy at the FLL melting transition, has been much focused on in recent experiments.[33,34,11,15,14] In Fig. 11, the entropy discontinuity at the first-order FLL melting transition is shown as a function of the flux-line density. The results obtained using the Hamiltonian in Eq. (1) are shown in filled circles. We find that the entropy discontinuity per flux line per layer $\Delta S(f) \sim 0.1 k_B$. The fact that ΔS is essentially independent of the applied magnetic field, *for the moderate anisotropy* $\Gamma=3$ *considered in this paper*, is consistent with the experimental results obtained by Schilling *et al.*[15] and Roulin *et al.*[14] They found $\Delta S(B) \sim 0.5 k_B$, independent of B. The values of $\Delta S=0.1 k_B$ are similar to the values found by Hu *et al.*[8] We attribute the difference between our values for $\Delta S(f) \sim 0.1 k_B$ and the experimental value $\Delta S(B) \sim 0.5 k_B$ to the difference in the anisotropy. YBCO has an anisotropy $\Gamma \sim 7$, while the anisotropy in this paper is $\Gamma=3$. As shown in our previous paper,[9] and also by Hu *et al.*,[8] the entropy jump at the FLL melting transition increases with increasing anisotropy.

To ensure that the artificial pinning potential introduced by the numerical mesh does not affect the FLL melting transition at $T_m(f)$, we must ensure that the helicity modulus perpendicular to the applied field vanishes at a temperature

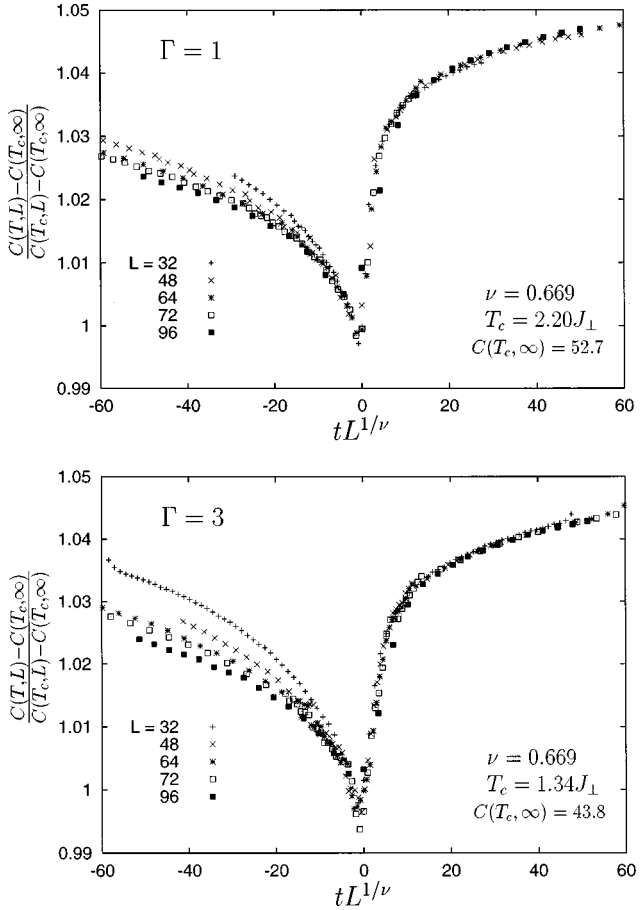

FIG. 9. Monte Carlo results for the specific heat of the anisotropic 3D XY model in zero magnetic field, for various system sizes $L\times L\times L$ with $L=32,48,64,72,96$, and two values of the anisotropy, $\Gamma=1$ and $\Gamma=3$, scaled according to Eq. (6). Here, $t=(T-T_c)/T_c$. The region of data collapse gives the width of the critical region. Note that this region is slightly wider for $\Gamma=3$ than for $\Gamma=1$.

$T_d(f)$ significantly below $T_m(f)$. Under such circumstances, the low-temperature phase for $T_d(f)<T<T_m(f)$ is characterized by a ''floating solid phase,'' mimicking the continuum limit. In Fig. 12, the helicity modulus along the x direction Υ_x is shown as a function of temperature for the same set of f used for the specific heat, structure function, and Υ_z. Figure 12 shows that for each flux-line density considered, Υ_x vanishes at a temperature $T_d(f)$ significantly lower than the corresponding FLL melting temperature $T_m(f)$. Thus, we have shown that in all systems considered in this paper, the depinning crossover at $T_d(f)$ does not affect the FLL melting at $T_m(f)\gg T_d(f)$. Although we have not shown it explicitly here, we have checked that $\Upsilon_y(T)$ is essentially identical to Υ_x, as required by symmetry.

In recent work,[35] it was pointed out that calculated entropy jumps ΔS at the melting transition of the Abrikosov vortex lattice could be brought into agreement with experiments[15] by introducing temperature-dependent parameters in the theory, reflecting fluctuations at a microscopic level surfacing in coarse-grained theories. The idea of using such a procedure was first introduced in Ref. 22 within the lowest Landau-level approach to the same problem, i.e., the high-field limit. This leads to an internal energy

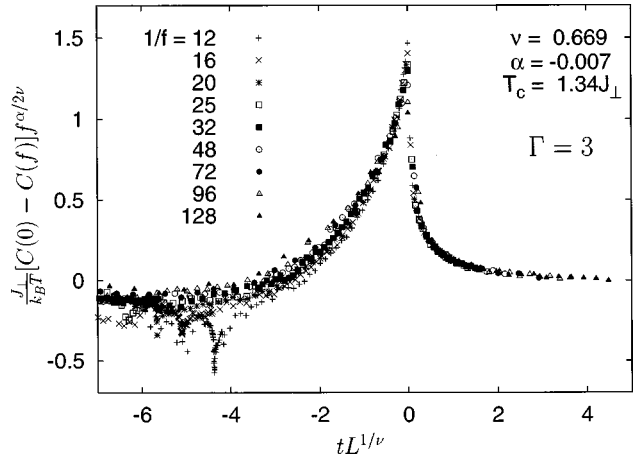

FIG. 10. Monte Carlo results for the specific heat of the anisotropic 3D XY model for a number of filling fractions f given by $1/f=12,\ldots,128$ with corresponding system sizes as explained in text, and anisotropy $\Gamma=3$, scaled according to Eq. (7). The results are in good agreement with the experimental results of Schilling *et al.* and Junod *et al.*

$$U(T)=\langle H\rangle - T\left\langle \frac{\partial H}{\partial T}\right\rangle, \tag{10}$$

where H is an effective T-dependent Hamiltonian, $\langle H\rangle = (1/Z)\Sigma H\exp(-H/k_BT)$, and $Z=\Sigma\exp(-H/k_BT)$ is the canonical partition function. For a derivation of this result, see the Appendix.

In extreme type-II superconductors, as modeled by the 3D XY model or the London model in the $\lambda\to\infty$ limit, the T dependence described above appears exclusively as a prefactor in the Hamiltonian $H=E_0(\tau)H_0$, where H_0 has no T-dependent prefactors, $\tau=T/T_{cMF}$ with T_{cMF} a mean-field zero-field transition temperature, and $E_0(\tau)=[\lambda(0)/\lambda(\tau)]^2$. H_0 is to be identified with the Hamiltonian used in this paper

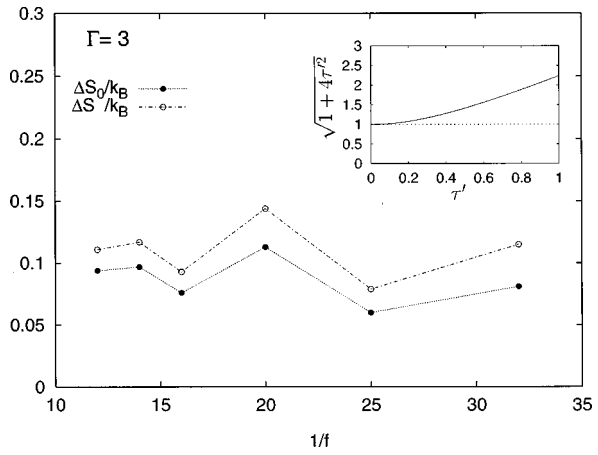

FIG. 11. The entropy jump per vortex line per layer $\Delta S(f)$ at the FLL melting transition for several vortex-line densities f. The filled circles represent the results obtained with a T-independent Hamiltonian, Eq. (1). The open circles represent the results obtained including a T-dependent prefactor in the Hamiltonian. We see that $\Delta S(f)$ essentially does not depend on f in this regime of filling fractions f, regardless of whether T-dependent prefactors are included in the Hamiltonian or not. The inset shows the enhancement factor in Eq. (14).

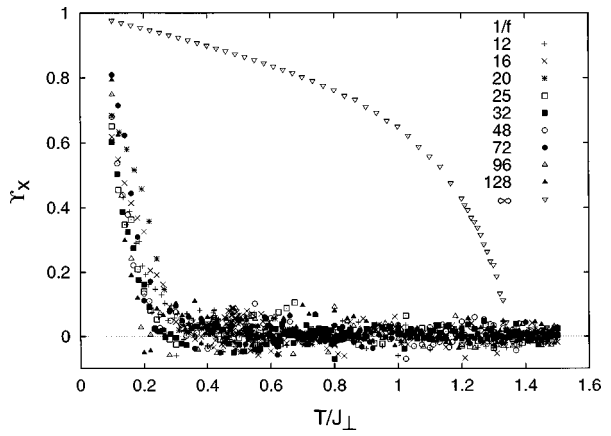

FIG. 12. The helicity modulus perpendicular to the field direction Υ_x as a function of temperature for several vortex-line densities f. For each f, Υ_x vanishes at a temperature $T_d(f)$ significantly lower than the corresponding FLL melting temperature $T_m(f)$. The artificial pinning potential of the numerical lattice therefore does not affect the FLL melting transition at $T_m(f) \gg T_d(f)$.

so far. For instance, in the two-fluid model $E_0(\tau)=1-\tau^4$, while the simplest mean-field approximation yields $E_0(\tau)=1-\tau$. Using the above, we find the internal energy given by

$$U=\left(E_0(\tau)-T\frac{dE_0(\tau)}{dT}\right)U_0(T'),$$

$$U_0(T')=\frac{1}{Z}\sum H_0\exp(-H_0/k_BT'), \tag{11}$$

$$T'=\frac{T}{E_0(\tau)}.$$

This leads to an entropy jump at the first-order melting transition of the Abrikosov vortex lattice

$$\Delta S=\frac{\Delta U}{T}=\left[E_0(\tau)-T\frac{dE_0(\tau)}{dT}\right]\frac{\Delta U_0(T')}{T}$$
$$=\frac{1}{E_0(\tau)}\left[E_0(\tau)-T\frac{dE_0(\tau)}{dT}\right]\Delta S_0(T'), \tag{12}$$

where $\Delta S_0(T')=\Delta U_0(T')/T'$ is the entropy jump obtained without any T-dependent parameters in the Hamiltonian, but where the quantity is to be evaluated at the temperature $T'=T/E_0(\tau)$. Note that the prefactor relating ΔS to ΔS_0 would always be 1 irrespective of what $E_0(\tau)$ is, if we had not included the contribution $-T\langle\partial H/\partial T\rangle$ to U. Using $E_0(\tau)=1-\tau^2$, we find

$$\Delta S(T)=\frac{1+\tau^2}{1-\tau^2}\Delta S_0(T'), \tag{13}$$

precisely as in Ref. 35. Note the difference in the arguments of $\Delta S(T)$ and $\Delta S_0(T')$. Reference 35 concludes that within a line-liquid model with moderate values of ΔS_0, substantially enhanced values for ΔS are obtained, particularly in the low-field regime, in agreement with experiments. The main factor in the enhancement is the denominator $1-\tau^2$, which vanishes as $T\to T_{cMF}$.

Note that the above procedure of substituting H_0 with $E_0(\tau)H_0$ does not in itself in any way assume that the physics of the vortex system in the low-field regime is determined exclusively by field-induced flux lines. However, were we to follow Ref. 35 and in addition assume that in the low-field regime there only exists one relevant length scale in the problem, namely, the magnetic length $a_0\sim 1/\sqrt{B}$, we *would* be assuming that only field-induced vortices are relevant degrees of freedom on the melting line. Our main point is that this may be questionable in the low-field regime, and we will therefore refrain from utilizing such an assumption.

If we insist on comparing $\Delta S_0(T')$ with results obtained using H_0, and not H,[35] then we must fix T' to values obtained for the melting line in such calculations. *Thus, τ cannot vary arbitrarily between* 0 *and* 1 *while fixing ΔS_0 independently.* Rather, τ and T' are related via $T'=T/E_0(\tau)$. In calculations of ΔS_0 using H_0, we must therefore have $T'/T_{cMF}<1$. Using $E_0(\tau)=1-\tau^2$, we find $\tau<(\sqrt{5}-1)/2$. This gives enhancement factors $(1+\tau^2)/(1-\tau^2)<\sqrt{5}$ within this model. If we express Eq. (13) in terms of $\tau'=T'/T_c$, we obtain

$$\Delta S=\sqrt{1+4\tau'^2}\Delta S_0(T'); \quad \tau'\in[0,1\rangle. \tag{14}$$

Similar enhancement factors may be found using the simplest mean-field approximation $E_0(\tau)=1-\tau$, that is, for instance, used in Ref. 30. It would yield an enhancement factor in Eq. (14) given by $1+\tau'$. In Fig. 11 we have also plotted the entropy jump as obtained using a T-dependent prefactor in the Hamiltonian. We have used the results obtained using H_0 and enhanced them by the prefactor in Eq. (14). The inset of the figure shows the enhancement factor on the melting line obtained in our simulations. It varies quite slowly as a function of τ' in the entire interval. Hence, even if we include the effect of $E_0(\tau)$ on ΔS, we obtain an essentially field-independent entropy jump in the field regime considered in Fig. 11. For specificity, we have chosen $E_0(\tau)=1-\tau^2$, and ignored the difference between T_c and the mean-field critical temperature. We note also in this context that Ref. 22 finds an entropy jump of the magnitude we have found here within the lowest Landau-level approximation. Furthermore, Ref. 29 finds similar results using the isotropic XY model with $f=1/6$, in agreement with earlier simulations of the same filling fraction.[18] Note the large difference in filling fractions between the present work and the work of Refs. 29 and 18. For $f=1/6$, commensuration effects due to the numerical lattice are severe, and could conceivably lead to overestimates of the magnitude of ΔS. This has been part of the motivation for pushing the simulations to the low filling fractions used in this paper.

E. *B*-*T* phase diagram

To estimate the real magnetic-field induction B corresponding to the flux-line densities considered in this paper, we use Eq. (8) and take $\xi_{ab}=12$–15 Å. With this value of ξ_{ab}, we find the magnetic field corresponding to the smallest flux-line densities considered ($f=1/128$) to be approxi-

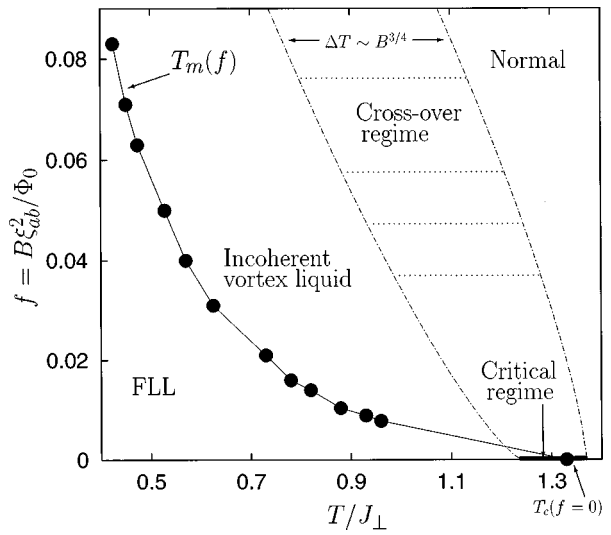

FIG. 13. The f-T phase diagram for the uniformly frustrated 3D XY model. The applied field is along the crystal c axis, the anisotropy parameter $\Gamma=3$. The FLL exhibits global phase coherence along the applied-field direction. The FLL phase is separated from the incoherent flux-line liquid phase by the melting line $T_m(f)$. The melting transition is a first-order phase transition with an entropy jump $\Delta S(f)\sim 0.1k_B$ for the anisotropy $\Gamma=3$ and field regime considered in this paper. In the incoherent vortex-liquid phase $T_m(f)<T<T_{Bc2}(f)$, there is only local, but no global, phase coherence in any direction. At finite fields, between the incoherent vortex liquid and the normal metal phase, there exists a broad crossover region where a blowout of thermally induced closed vortex loops takes place, eventually also destroying superconductivity on short length scales. The width of the crossover regime is obtained from scaling behavior of the specific heat. Another, consistent, method of obtaining this width, is to estimate the temperature regime, which correponds to an uncertainty of 10% in the maximum value of the specific-heat anomaly at $T_{Bc2}(f)$. Since this anomaly becomes broader with increasing field, the crossover region becomes wider. This is also confirmed from the scaling results for the specific heat.

mately 5–7 T. In Fig. 13 we show the f-T phase diagram originating from simulations of the XY model. The flux-line densities f considered are $1/f=12,14,16,20,25,32,48,64,72,84,96,112,128$. We see that the overall behavior of this phase diagram is consistent with the phase diagram in YBCO measured by Schilling *et al.*[15] and Junod *et al.*[14] The FLL melting line at $T_m(f)$ separates the superconducting Abrikosov FLL phase from the incoherent vortex liquid phase, the latter being characterized by finite resistivity and strong diamagnetic fluctuations, with simultaneous loss of Bragg peaks in the FLL structure factor, flux-line integrity, and global phase coherence in all directions. The remains of the zero-field vortex loop ''blowout'' around $T_{Bc2}(f)$ destroys phase coherence on all length scales, and thus separates the incoherent vortex liquid phase from the normal metal phase. The melting line $T_m(f)$ decreases with decreasing f with a positive curvature. Note also that the width of the critical region is large enough to influence the FLL melting transition over a sizable field range. This field range is seen to extend up to $f\approx 1/256$, which we may conservatively estimate to be at least of order 0–1 T.

V. CONCLUSION

In this paper, we have investigated characteristics of the molten phase of the Abrikosov flux-line lattice via Monte Carlo simulations on the three-dimensional uniformly frustrated XY model. Bragg peaks in the static structure factor and phase coherence along the direction of the applied magnetic field are both lost simultaneously, rendering the vortex liquid phase incoherent. This behavior is triggered by thermal excitations of closed vortex loops of diameters of the order of the average distance between flux lines in the low-temperature lattice phase. On the melting line, this mechanism suffices to produce highly nontrivial vortex configurations with appreciable statistical weight *on the template of field-induced vortices.* These configurations are characterized by a ''percolation'' of closed vortex loops threading the entire sample in any direction. In particular, this is the case for directions transverse to the direction of the applied magnetic field, which is tantamount to a loss of line tension of the field-induced flux lines. It renders a picture of the molten phase of the flux-line lattice in terms of a liquid of well-defined, separated, and directed line objects, invalid. Equivalently, a picture in terms of world lines of 2D nonrelativistic superfluid bosons is invalid in the liquid phase. An effective theory of the flux-line lattice melting and the vortex-liquid phase thus appears to present a formidable challenge involving the solution of a self-consistent coupled theory of field-induced flux-line objects, and thermally induced closed vortex loops.[6–8] This coupling must evidently render the flux-line tension equal to zero in the liquid phase. Unfortunately, it is therefore doubtful that the intuitively appealing physics of directed polymers is particularly relevant for the vortex-liquid phase.

Scaling functions for the specific heat are calculated, both in zero and finite magnetic field. The zero-field results yield a sizable critical region $|T-T_c|/T_c\approx 0.1$, corroborating the notion that critical fluctuations of extreme type-II superconductors, i.e., vortex loops, will influence such phenomena as flux-line lattice melting over an appreciable range of magnetic inductions, possibly up to fields of order 1 T in moderately anisotropic superconductors. The field range will depend on mass anisotropy, since the width of the critical region and the low-field shape of the melting curve both appear to be influenced by the layeredness of the superconductor.

The finite-field results for the scaling functions for the specific heat, as well as the obtained phase diagram for an anisotropy parameter $\Gamma=3$, are consistent with experiments on the slightly more anisotropic cuprate high-T_c superconductor YBCO, with $\Gamma\approx 7$.

Finally, we note that columnar defects will not be particularly efficient in enhancing the critical current density in a superconductor where the FLL melting line is strongly influenced by thermally excited closed vortex loops. (The influence of columnar defects on the vortex system was studied using Monte Carlo simulations in Ref. 36 for a filling fraction $f=1/2$.) The vortex-loop susceptibility should be sensitive to the phase-stiffness of the superconductor. The phase stiffness is in turn largely controlled by the superfluid density, and therefore also by the charge-carrier density. In order to avoid the detrimental effects on transport properties in

high-T_c superconductors from a vortex-loop ''blowout,'' an increase of the charge-carrier density appears to be essential.

ACKNOWLEDGMENTS

Support from the Research Council of Norway (Norges Forskningsråd) under Grants No. 110566/410 and No. 110569/410, as well as a grant for computing time under the Program for Super-computing, is gratefully acknowledged. We thank S.-K. Chin, A. Hansen, J. S. Høye, A. E. Koshelev, and Z. Tešanović for discussions. J. Amundsen is acknowledged for assistance in optimizing our computer codes for use on the Cray T3E.

APPENDIX: INTERNAL ENERGY

In this appendix, we give a brief derivation of a generalized expression for the internal energy of a system with an effective T-dependent Hamiltonian. Consider a system in the canonical ensemble. For illustration, we will consider the well-known (P,V,T) system. Our result for the internal energy U does not depend on the nature of the work term. The system has a statistical distribution function given by the canonical law

$$\rho=\frac{1}{Z}e^{-H/\theta}, \tag{A1}$$

where the normalization constant Z is the canonical partition function

$$Z=\sum_{\text{configurations}} e^{-H/\theta}, \tag{A2}$$

where θ is a parameter of the distribution function that remains to be determined, such that

$$\sum_{\text{configurations}} \rho=1. \tag{A3}$$

We insist that this normalization is to be maintained if the parameters V and θ are varied differentially. The Hamiltonian and hence the partition function will depend on V through the wall potential of the problem. Let us, arbitrarily, write the partition function in the following way:

$$Z=e^{-\Psi/\theta}, \tag{A4}$$

where Ψ is a system-dependent parameter that also remains to be determined. When $V\to V+dV$ and $\theta\to\theta+d\theta$, we will therefore also need to vary $\Psi\to\Psi+d\Psi$ in order to maintain correct normalization of ρ. Hence, we have

$$\sum e^{[\Psi-H(V,\theta)]/\theta}=1=\sum e^{[\Psi+d\Psi-H(V+dV,\theta+d\theta)]/(\theta+d\theta)}. \tag{A5}$$

Note that we have allowed H to depend on the statistical parameter θ. Expanding to first order in all differentials, we obtain

$$\sum e^{[\Psi-H(V,\theta)]/\theta}\left\{1+\frac{1}{\theta}\left[d\Psi-\left(\frac{\partial H}{\partial V}dV+\frac{\partial H}{\partial\theta}d\theta\right)-\frac{d\theta}{\theta}(\Psi-H)\right]\right\}=1. \tag{A6}$$

Since the orginal distribution prior to changing $V\to V+dV$ and $\theta\to\theta+d\theta$ also was normalized we obtain the following constraint on the differentials dV, $d\theta$, and $d\Psi$:

$$d\Psi=\frac{d\theta}{\theta}\left[\Psi-\langle H\rangle+\theta\left\langle\frac{\partial H}{\partial\theta}\right\rangle\right]+\left\langle\frac{\partial H}{\partial V}\right\rangle dV. \tag{A7}$$

Here, $\langle\vdots\rangle$ denotes a statistical average with respect to the original distribution function $\exp[(\Psi-H)/\theta]$. In order to make the connection to thermodynamics, we now compare the above with the ''thermodynamic identity''

$$dF=-SdT-PdV=\frac{dT}{T}(F-U)-PdV, \tag{A8}$$

where $F=U-TS$ is Helmholz free energy, S is the entropy, and U is the internal energy. This comparison yields directly

$$P=\left\langle-\frac{\partial H}{\partial V}\right\rangle,$$

$$\frac{d\theta}{\theta}=\frac{dT}{T}\to\theta=k_BT, \tag{A9}$$

$$\Psi=F,$$

$$U=\langle H\rangle-T\left\langle\frac{\partial H}{\partial T}\right\rangle.$$

Note that Ψ thus identified is the only choice consistent with $F=-k_BT\ln Z$. This then fixes U. Also, the expression for U obtained in this fashion is identical to that obtained directly from the usual relation

$$U=-\frac{\partial\ln Z}{\partial\beta}, \tag{A10}$$

with an assumed T-dependent Hamiltonian.

[1] P. L. Gammel, D. J. Bishop, G. J. Dolan, J. R. Kwo, C. A. Murray, L. F. Schneemeyer, and J. V. Waszczak, Phys. Rev. Lett. **59**, 2592 (1987); **61**, 1666 (1988).

[2] D. R. Nelson, Phys. Rev. Lett. **60**, 1973 (1988); D. R. Nelson and H. S. Seung, Phys. Rev. B **39**, 9153 (1989).

[3] G. Eilenberger, Phys. Rev. **153**, 584 (1967).

[4] A. Houghton, R. A. Pelcovits, and A. Sudbø, Phys. Rev. B **40**, 6763 (1989).

[5] A. A. Abrikosov, Zh. Eksp. Teor. Fiz. **32**, 1442 (1957) [Sov. Phys. JETP **5**, 1174 (1957)].

[6] Z. Tešanović, Phys. Rev. B **51**, 16 204 (1995).

[7] A. K. Nguyen, A. Sudbø, and R. E. Hetzel, Phys. Rev. Lett. **77**, 1592 (1996).

[8] X. Hu, S. Miyashita, and M. Tachiki, Phys. Rev. Lett. **79**, 3498 (1997).

[9] A. K. Nguyen and A. Sudbø, Phys. Rev. B **57**, 3123 (1998).

[10] T. J. Hagenaars and E. H. Brandt, Phys. Rev. B **56**, 11 435 (1997).
[11] E. Zeldov, D. Majer, M. Konczykowski, V. B. Geshkenbein, V. M. Vinokur, and H. Shtrikman, Nature (London) **375**, 373 (1995); N. Morozov, E. Zeldov, D. Majer, and M. Konczykowski, Phys. Rev. B **54**, R3784 (1996); D. T. Fuchs, R. A. Doyle, E. Zeldov, D. Majer, W. S. Seow, R. J. Drost, T. Tamegai, S. Ooi, M. Konczykowski, and P. H. Kes, *ibid.* **55**, R6156 (1997).
[12] M. V. Feigel'man, V. B. Geshkenbein, L. B. Ioffe, and A. I. Larkin, Phys. Rev. B **48**, 16 641 (1993).
[13] M. B. Salamon, J. Shi, N. Overend, and M. A. Howson, Phys. Rev. B **47**, 5520 (1993).
[14] M. Roulin, A. Junod, A. Erb, and E. Walker, J. Low Temp. Phys. **105**, 1099 (1996); A. Junod, M. Roulin, J. Y. Genoud, B. Revaz, A. Erb, and E. Walker, Physica C **275**, 245 (1997); M. Roulin, A. Junod, and E. Walker, Science **273**, 1210 (1996); Physica C **282**, 1401 (1997).
[15] A. Schilling, R. A. Fisher, N. E. Phillips, U. Welp, D. Dasgupta, W. K. Kwok, and G. W. Crabtree, Nature (London) **382**, 791 (1996).
[16] O. Jeandupeux, A. Schilling, H. R. Ott, and A. van Otterlo, Phys. Rev. B **53**, 12 475 (1996); A. Schilling, R. A. Fisher, N. E. Phillips, U. Welp, W. K. Kwok, and G. W. Crabtree, Phys. Rev. Lett. **78**, 4833 (1997).
[17] We thank Z. Tešanović for discussions on this point.
[18] R. E. Hetzel, A. Sudbø, and D. A. Huse, Phys. Rev. Lett. **69**, 518 (1992).
[19] Ying-Hong Li and S. Teitel, Phys. Rev. B **47**, 359 (1993); **49**, 4136 (1994).
[20] T. Chen and S. Teitel, Phys. Rev. B **55**, 11 766 (1997).
[21] R. Cavalcanti, G. Carneiro, and A. Gartner, Europhys. Lett. **17**, 449 (1992); G. Carneiro, R. Cavalcanti, and A. Gartner, Phys. Rev. B **47**, 5263 (1993).
[22] J. Hu and A. H. MacDonald, Phys. Rev. B **56**, 2788 (1997).
[23] C. Dasgupta and B. I. Halperin, Phys. Rev. Lett. **47**, 1556 (1981).
[24] L. Onsager, Nuovo Cimento Suppl. **6**, 249 (1949); P. C. Hemmer, H. Holden, and S. K. Ratkje, *The Collected Works of Lars Onsager* (World Scientific, Singapore, 1996), p. 1070.
[25] N. Goldenfeld, *Lectures on Phase Transitions and the Renormalization Group* (Addison-Wesley, Reading, MA, 1992).
[26] N. Schultka and E. Manousakis, Phys. Rev. B **52**, 7528 (1995); See also M. Friesen and P. Muzikar, cond-mat/9703135 (unpublished).
[27] M. Franz and S. Teitel, Phys. Rev. Lett. **73**, 480 (1994); S. A. Hattel and J. M. Wheatley, Phys. Rev. B **50**, 16 590 (1994); **51**, 11 951 (1995).
[28] M. Kiometzis, H. Kleinert, and A. M. J. Schakel, Fortschr. Phys. **43**, 697 (1995); cond-mat/9708142 (unpublished).
[29] S. Ryu and D. Stroud, Phys. Rev. Lett. **78**, 4629 (1997).
[30] A. E. Koshelev, Phys. Rev. B **56**, 11 201 (1997).
[31] B. A. Huberman and S. Doniach, Phys. Rev. Lett. **43**, 950 (1979); D. S. Fisher, Phys. Rev. B **22**, 1190 (1980).
[32] V. J. Emery and S. A. Kivelson, Nature (London) **374**, 434 (1995).
[33] H. Safar, P. L. Gammel, D. A. Huse, D. J. Bishop, J. P. Rice, and D. M. Ginsberg, Phys. Rev. Lett. **69**, 824 (1992).
[34] H. Pastoriza, M. F. Goffman, A. Arribére, and F. de la Cruz, Phys. Rev. Lett. **72**, 2951 (1994).
[35] M. J. W. Dodgson, V. B. Geshkenbein, H. Nordborg, and G. Blatter, Phys. Rev. Lett. **80**, 837 (1998); Phys. Rev. B **57** 14 498 (1998).
[36] M. Wallin and S. M. Girvin, Phys. Rev. B **47**, 14 642 (1993).